http://dx.doi.org/10.11142/jicems.2014.3.1.7
Journal of International Conference on Electrical Machines and Systems Vol. 3, No. 1, pp. 7~14, 2014

Transient Simulation Studies of Squirrel-Cage Induction Motor Directly Supplied with Aircraft Variable Frequency Power

Xiaofei Du *, Deqiang Wang *, and Yuanjun Zhou *

Abstract – Aircraft variable frequency power and a new application of induction motor under the aero-power are introduced. The transient models and simulation of induction motor are reviewed. A new transient model and simulation method is presented that includes deep-bar effect and magnetic saturation. Dynamic magnetizing inductance, rotor resistance and leakage reactance are considered as varying parameters in state-space model. Base on known rotor structure and speed, these parameters can be calculated.

Keywords: Aircraft variable frequency power, Induction motor, Transient simulation, Deep bar, Skin effect, Magnetic saturation

Nomenclature

i_s	stator current
i_r	rotor current
i_{sd}	stator d-axis current in Park variables
i_{sq}	stator q-axis current in Park variables
i_{rd}	rotor d-axis current in Park variables
i_{rq}	rotor q-axis current in Park variables
J	inertia of motor rotor
P	number of pair of poles
F_m	friction factor of induction motor
R_s	stator resistance per phase
R_r	rotor resistance per phase
s	slip
T_e	electromechanical torque
T_L	load torque
v_s	stator voltage
v_{sd}	stator d-axis voltage in Park variables
v_{sq}	stator q-axis voltage in Park variables
v_r	rotor voltage
ω_r	mechanical angular speed
ω	rated synchronous angular speed
$X_{\sigma s}$	stator leakage reactance and stator inductance per phase
X_m, L_m	magnetising reactance and inductance per phase
$X_{\sigma r}$	rotor leakage reactance

* Dept. of Electrical Engineering, BEIHANG University, CHINA. (xfdu@asee.buaa.edu.cn ,deqiangwang1988@gmail.com zhouyuanjun@buaa.edu.cn)

Received 13 October 2013 ; Accepted 28 November 2013

1. Introduction

The continual studies have contributed to More Electrical Aircraft (MEA) since the early 1980's [1]. The technology of More Electrical Aircraft adopts increasingly electrical power to drive other aircraft secondary power systems, including mechanical, hydraulic and pneumatic. In the progress of MEA, variable frequency AC power supply, one predominant technology for MEA, has been applied on large civil aircrafts [2]-[4]. Different from conventional aircraft AC power supply, variable frequency generators output frequency ranging from 360 to 800 Hz. And the voltage of the generators is regulated to a constant value.

The background of this article is to develop a potential application of induction motor with strong structure, high reliability and low cost, as the pump drive in the MEA [5][6]. In the circumstance, induction motors work at a wide range of input frequency from 360 to 800 Hz [7].

The aim of the article focus on modeling and simulating the transient of deep-bar induction motors under the supply of aerospace variable frequency power. The work also provides advices to the structure design of deep-bar rotors. Due to skin effect of deep-bar, the resistance and leakage reactance of rotor vary as the rotor frequency changes during the transient operation. With rotor speed increasing and rotor frequency decreasing, the rotor resistance

becomes lower and leakage reactance higher [8]. Consequently the starting and frequency-changing performances are affected by the varying-parameters. The effect is even more obvious under the aerospace power supply frequency than civil power frequency with 50 Hz.

Recently many researchers have analyzed and modified the transient models of squirrel-cage induction machine to get much more accurate approaches [9]-[15]. Classical model of the rotor deep-bar is based on transmission line theory, by which each deep bar is divided into equal or unequal sections along the depth of each rotor slot. Accordingly the conventional equivalent T-circuit of induction motor modifies the branch of rotor into multiple branches in parallel. Varity of improved equivalent circuits, including L-circuit, PI-circuit and improved PI-circuit, were discussed [9] in order to obtain accurate model configuration with less parallel branches and acceptable error. Another unequal separation concerned optimized separation proportion to achieve more suitable equivalent branches with less error [13]. Based on the modified equivalent T-circuit, squirrel-cage induction motor transient performance was analyzed [11][14][16]. By calculating the dynamic rotor resistance and leakage reactance, transient simulation was also presented [17].

The main contribution of this article will be that the author proposes a new approach without adding extra rotor branches of equivalent circuit for the transient simulation on squirrel-cage induction motor considering skin effect and magnetic saturation. The transient simulation includes starting and frequency-changing process, of which the latter is particularly for aerospace variable-frequency power supply. Tracing the rotor speed and frequency, varying rotor resistance and leakage reactance can be calculated with the known rotor structure and frequency. Magnetic saturation effect can be acquired from varying magnetising inductance. Similarly magnetising inductance can be calculated through tracing rotor speed and magnetic current. So both rotor parameters and magnetising inductance can be regard as frequency-dependent parameters. Inducing these frequency-dependent parameters into state-space model, a new transient model and simulation can be obtained.

2. A Modified Transient Induction Motor Model

The traditional equations of three-phase induction motor with squirrel-cage bars are based on steady-state equivalent circuit. In order to approach dynamic model, many different methods were introduced to modify the equivalent circuit, e.g. using double-cage type circuit and more rotor branches. Most of them result in dimension increase of the equations. Although motor parameters vary because of skin effect and magnetizing saturation, the dynamic model can be established by adding these varying parameters directly into the steady model. As pointed out in Fig. 1, magnetising inductance, rotor leakage reactance and resistance are not constant during the transient process. Based on the circuit with variable parameters, steady state-space equations of induction motors can be modified.

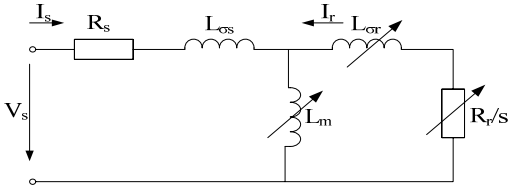

Fig. 1. Equivalent circuit of squirrel-cage induction motor including skin effect and magnetizing saturation

Traditional voltage and electromagnetic torque equations for induction motors are represented as below.

$$\begin{aligned} v_s &= R_s i_s + \frac{d\psi_s}{dt} + j\omega\psi_s \\ v_r &= R_r i_r + \frac{d\psi_r}{dt} + js\omega\psi_r \\ T_e &= PL_m \operatorname{Im}\left(i_s i_r^*\right) \end{aligned} \tag{1}$$

And mechanical equation is also denoted by (2).

$$T_e - T_L - F_m\omega_r = \frac{J}{P}\frac{d\omega_r}{dt} \tag{2}$$

In (1), ψ_s represents stator flux linkage and ψ_r rotor flux linkage.

$$\left.\begin{aligned} \psi_s &= L_s i_s + L_m i_r \\ \psi_r &= L_m i_s + L_r i_r \end{aligned}\right\} \tag{3}$$

where

$$\left.\begin{aligned} L_s &= \left(X_{\sigma s} + X_m\right)/\omega \\ L_r &= \left(X_m + X_{\sigma r}\right)/\omega \\ \frac{d\psi_s}{dt} &= \frac{dL_s}{dt} i_s + L_s\frac{di_s}{dt} + \frac{dL_m}{dt} i_r + L_m\frac{di_r}{dt} \\ \frac{d\psi_r}{dt} &= \frac{dL_m}{dt} i_s + L_m\frac{di_s}{dt} + \frac{dL_r}{dt} i_r + L_r\frac{di_r}{dt} \end{aligned}\right\} \tag{4}$$

Before substituting (3) into (1), two differential equations should be calculated by

Adopting (4) to substitute the differential flux linkage of stator and rotor in (1), modified voltage equation are obtained.

$$v_s = R_s i_s + i_s pL_s + L_s pi_s + i_r pL_m + L_m pi_r + j\omega\left(L_s i_s + L_m i_r\right) \quad (5)$$
$$v_r = R_r i_r + i_s pL_m + L_m pi_s + i_r pL_r + L_r pi_r + js\omega\left(L_m i_s + L_r i_r\right)$$

where $p = \frac{d}{dt}$.

For steady-state equations, classical two-axis model in d-q stationary reference frame ensure that the inductance coefficients are independent of rotor position, i.e. the motor parameters are constant in d-q frame at stable rotation state. However, transient equations still incudes variable parameters. These varying parameters can be represented by differential operator in following state-space equations.

$$\left.\begin{aligned} v_s &= v_{sd} + jv_{sq} \\ v_r &= v_{rd} + jv_{rq} \\ i_s &= i_{sd} + ji_{sq} \\ i_r &= i_{rd} + ji_{rq} \end{aligned}\right\} \quad (6)$$

Deducing from simultaneous equations with (5) and (6), dynamic state-space equations can be written as.

$$\begin{bmatrix} v_{sd} \\ v_{sq} \\ v_{rd} \\ v_{rq} \end{bmatrix} = \begin{bmatrix} R_s + pL_s + L_s p & -L_s\omega & pL_m + L_m p & -L_m\omega \\ L_s\omega & R_s + pL_s + L_s p & L_m\omega & pL_m + L_m p \\ pL_m + L_m p & -L_m s\omega & R_r + pL_r + L_r p & -L_r s\omega \\ L_m s\omega & pL_m + L_m p & L_r s\omega & R_r + pL_r + L_r p \end{bmatrix} \begin{bmatrix} i_{sd} \\ i_{sq} \\ i_{rd} \\ i_{rq} \end{bmatrix} \quad (7)$$

For simplifying the expression of state-space equations, (7) could be expressed as follows.

$$\begin{bmatrix} [V_s] \\ [V_r] \end{bmatrix} = [R]\begin{bmatrix} [i_s] \\ [i_r] \end{bmatrix} + [L]\, p\begin{bmatrix} [i_s] \\ [i_r] \end{bmatrix} + \omega_r P[G]\begin{bmatrix} [i_s] \\ [i_r] \end{bmatrix} \quad (8)$$

And deducing from (8), current differential equation is written.

$$p\begin{bmatrix} [i_s] \\ [i_r] \end{bmatrix} = [L]^{-1}\left(-[R] - \omega_r P[G]\right)\begin{bmatrix} [i_s] \\ [i_r] \end{bmatrix} + [L]^{-1}\begin{bmatrix} [V_s] \\ [V_r] \end{bmatrix} \quad (9)$$

$$p\begin{bmatrix} [i_s] \\ [i_r] \end{bmatrix} = [L]^{-1}[R]\begin{bmatrix} [i_s] \\ [i_r] \end{bmatrix} + [L]^{-1}\begin{bmatrix} [V_s] \\ [V_r] \end{bmatrix}$$

where,

$$[L] = \begin{bmatrix} L_s & & L_m & \\ & L_s & & L_m \\ L_m & & L_r & \\ & L_m & & L_r \end{bmatrix}$$

$$[R] = -\begin{bmatrix} R_s + pL_s & -L_s\omega & pL_m & -L_m\omega \\ L_s\omega & R_s + pL_s & L_m\omega & pL_m \\ pL_m & -L_m s\omega & R_r + pL_r & -L_r s\omega \\ L_m s\omega & pL_m & L_r s\omega & R_r + pL_r \end{bmatrix}.$$

3. Skin Effect and Magnetising Saturation

3.1 Deep Bar Effect

Deep bar effect contributes to the rotor cage presenting different impedance during transient periods. The reason for the difference lies, in essence, in the nonlinear behaviors of rotor. When it operates at stable speed, the rotor frequency keeps constant and accordingly the penetration depth which affects rotor impedance is a fixed value. When rotor frequency changes during transient periods, the depth is different, i.e. the impedance of rotor depends on the transient rotor frequency.

The proposed method illustrates dynamic process by using the variation in the rotor impedance over a specified frequency range. The frequency range is in reference to operation conditions that hereinafter refer to aerospace power frequency ranging from 360 Hz to 800 Hz. As the power frequency higher than industrial frequency with 50 Hz, the more obvious skin effect can be attributed to variable frequency during dynamic periods.

With known structure of deep bar, the skin effect can be acquired through analyzing dynamic process of rotor impedance, including slot leakage reactance and resistance. The analysis is described with rectangular slot.

Without considering skin effect, the resistance and slot leakage reactance are given as

$$\left.\begin{aligned} R_{=} &= \frac{\rho l}{A} = \frac{\rho l}{bh} \\ L_{=} &= \mu_0 l \frac{h}{b} \end{aligned}\right\} \quad (10)$$

where,

A the area of rotor bar
l axis length of machine's magnetic circuit
b width of bar
h depth of bar
ρ resistivity
μ_0 permeability of vacuum.

Considering skin effect, the impedance of rectangular bar at different frequency is expressed below:

$$\left.\begin{aligned} R_{\approx} &= K_R R_{=} \\ L_{\approx} &= K_L L_{=} \end{aligned}\right\} \tag{11}$$

And K_R and K_L represent changing rates of resist-a nce and slot leakage inductance respectively.

$$\begin{aligned} K_R &= \xi \frac{sh2\xi + \sin 2\xi}{ch2\xi - \cos 2\xi} \\ K_L &= \frac{3}{2\xi} \frac{sh2\xi - \sin 2\xi}{ch2\xi - \cos 2\xi} \end{aligned} \tag{12}$$

where,

$$\xi = \sqrt{\frac{b}{b_s} \pi \mu_0 f_r \sigma} \cdot h \approx \sqrt{\pi \mu_0 f_r \sigma} \cdot h$$

$f_r = s f_s$ rotor frequency
$\sigma = \rho^{-1}$ conductivity coefficient of bar

During transient process of variable frequency, rotor impedance is not fixed and changes as varying frequency. The calculation of dynamic impedance is showed above by using available design data about rotor structure and the known frequency range. Based on the information, dynamic rotor impedance can be determined, e.g. the process shown in Fig. 2.

3.1 Magnetic Saturation

The magnetic reluctance of materials results in the permeability decreases with magnetizing current increasing to a certain degree. Magnetic saturation of the main flux contributes to the varying of magnetizing inductance. The magnetizing inductance, in this case, can be regarded as a function of magnetising current. The functional relation between magnetising inductance and current can be obtained from no-load tests that hold in different voltage levels. Because magnetic saturation is based on the structure and material characteristics, magnetising inductance can also be calculated through Finite Element Analysis with known design data. So by this method magnetising inductance is described as a frequency-dependent function, showing the dynamic inductance versus slip or rotor frequency.

The FEA methods help designers to analyze the saturation situation of designed machines. However manufacturing errors could cause the difference between FEA results and motor tests at times. So magnetising inductance is also obtained from no-load tests. Fig. 3 represents the magnetising reactance varies versus the current. The functional relation in Fig. 3 can be established by curve approximation methods.

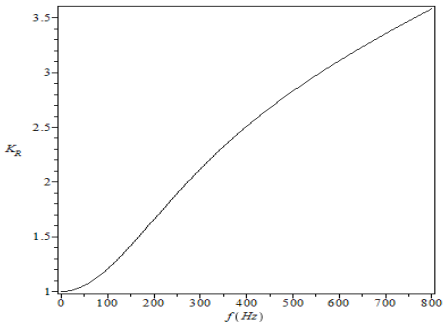

(a) K_R

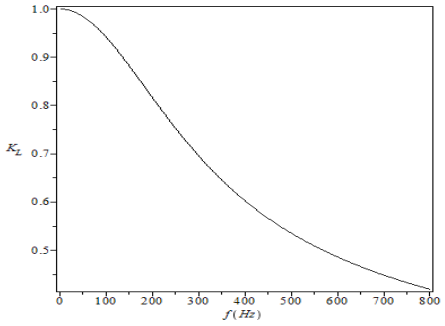

(b) K_L

Fig. 2. Rotor impedance varies versus frequency within 800 Hz, a 7.5 kW induction motor. (a) and (b) represent changing rate of resistance and slot leakage inductance respectively

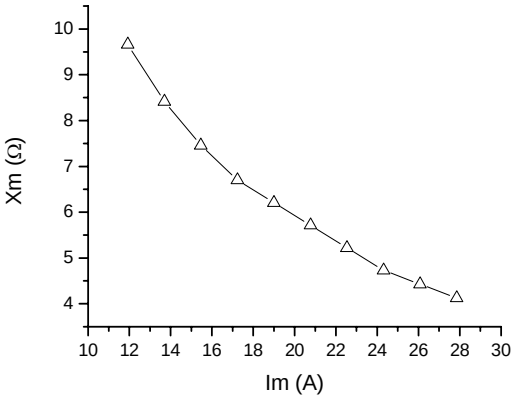

Fig. 3. Variation of magnetizing reactance versus magnetizing current

4. Transient Simulations

4.1 Simulation Model Configuration

The mathematical model of squirrel cage induction motors is based on the d-q stationary reference frame. The simulations are achieved in the Matlab/Simulink environment. Detailed model configuration is described in Fig.4.

Deep bar effect and magnetic saturation are considered in the simulation model through introducing variable rotor impedance and magnetising inductance into voltage-current equations. And varying magnetising inductance is also contained in torque equation. As shown in Fig. 4, varying rotor parameters are given by calculating the design data about rotor structure and tracing rotor speed or frequency. Although magnetising inductance can be regarded as a function of frequency-dependent during starting periods, it is obtained, in the model, by using the function of magnetising current. The calculation methods of variable parameters are presented in section 3.

4.2 Starting Process

The design and no-load test data of a 7.5 kW deep bar induction motor were used in the simulation model. The aerospace supply power for this motor has constant voltage of 115 volt and variable frequency ranging from 360 Hz to 800 Hz. Because higher frequency shows more obvious deep bar effect, the simulation results at 800 Hz are demonstrated below. Detailed motor data are shown in Table 1. During the starting process, the rotor impedance varied as rotor speed. The varying process about rotor parameters is represented in Fig. 5. From Fig. 6 to Fig. 8, the comparison of two kinds of calculation is presented, of which one calculated deep bar effect and main flux saturation, and another used constant motor parameters. Deep bar effect and magnetic saturation improve the starting performance evidently, of which start torque got higher and starting current lower.

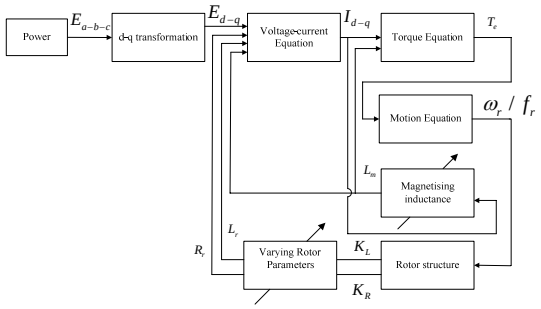

Fig. 4. Schematic of the simulation model

Table 1. Specification of a 7.5 kw Motor

Output	7.5 kW	No. of Poles	4
Voltage	115 V	Frequency range	360-800Hz
Inertia of motor rotor		0.00627 kg.m^2	
Equivalent circuit constant (rated)			
Rs (per phase)		0.08 Ω	
Ls (per phase)		1.566e-04 H	
Rr (per phase)		0.063 Ω	
L_r (slot leakage inductance)		1.133e-04 H	

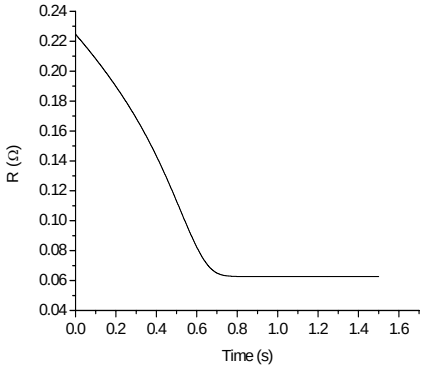

(a)

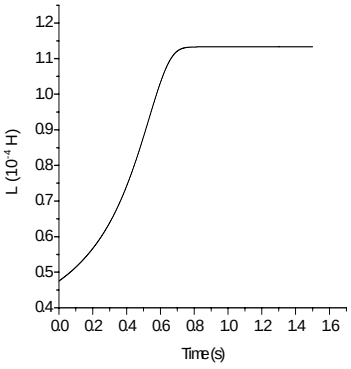

(b)

Fig. 5. Variable rotor impedance in starting process. (a) and (b) represent rotor resistance and slot inductance respectively

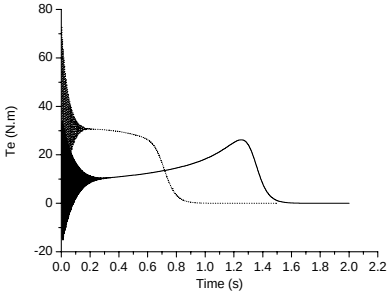

Fig. 6. Torque comparison of simulations results with constant parameters (solid) and with representing skin effect and saturation (dashed)

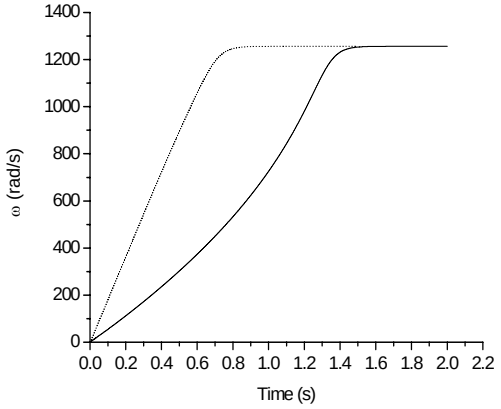

Fig. 7. Rotor speed comparison of simulations results with constant parameters (solid) and with representing skin effect and saturation (dashed)

As the output speed of aero engines changes, the power system frequency falls down at a defined rate of 200 Hz/s from 800 Hz to 600 Hz [7]. The effect under this condition has been analyzed through adding a frequency controller in the simulation model.

As shown in Fig. 9, frequency decreases from 800 Hz at the point (1.5 sec.) when motors operate at steady state to 600 Hz within 1 second. During the period of frequency change, motor performance shows nonlinear features. As the motor impedance vary which affected by frequency change, e.g. rotor impedance in Fig. 10, dynamic torque, speed and stator current are simulated in Fig. 11.

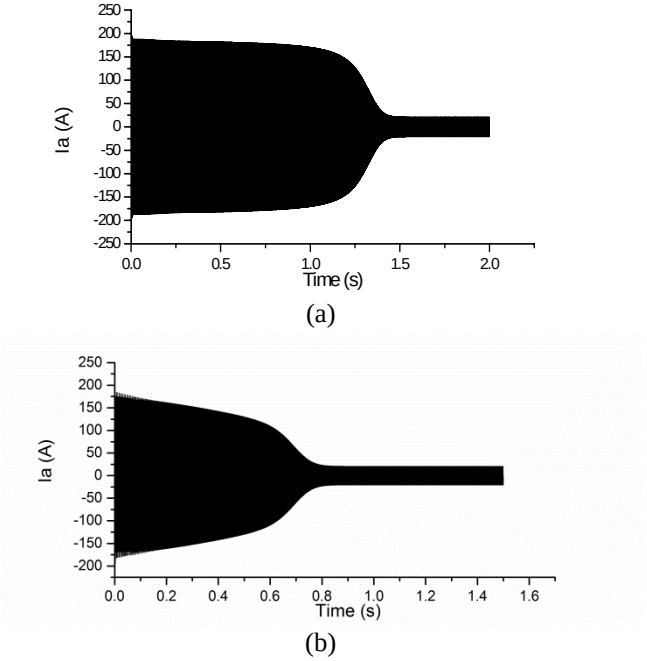

Fig. 8. Stator phase current comparison of simulations results with constant parameters (a) and with representing skin effect and saturation (b)

4.3 A 200 Hz/s Frequency change

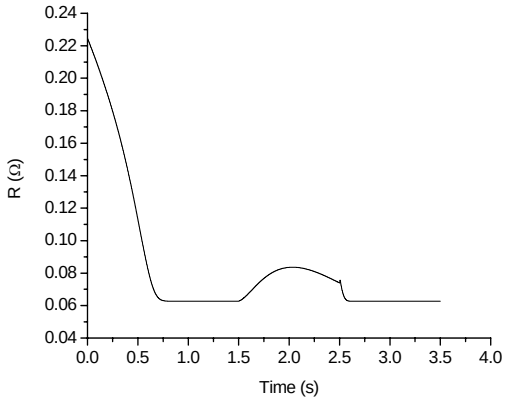

(a)

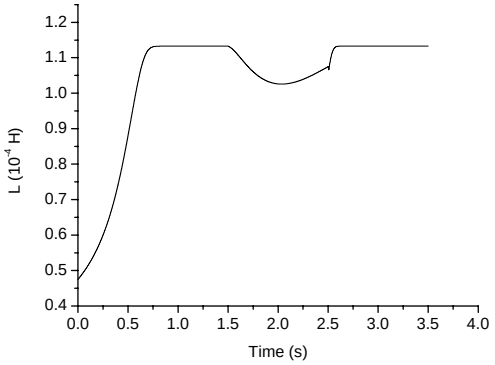

(b)

Fig. 9. Variable rotor impedance for frequency change. (a) and (b) represent rotor resistance and slot inductance respectively

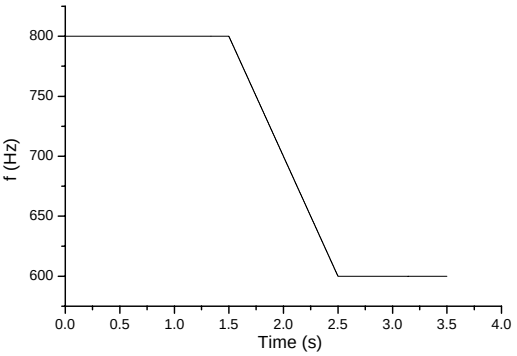

Fig. 10. A 200 Hz/s frequency change

5. Conclusion

A transient simulation model is demonstrated for a squirrel cage induction motor that includes deep bar effect and magnetic saturation in the main flux. The method uses

the data of known rotor structure and no-load tests. For designers, the simulation helps to analyze the desired rotor structure with deep bar, which could improve the transient performance of induction motors. Without no-load experiments, variable magnetizing inductance also can be built by FEA methods, which is suitable during design process. The proposed simulation model can also be used to analyze dynamic process for frequency change.

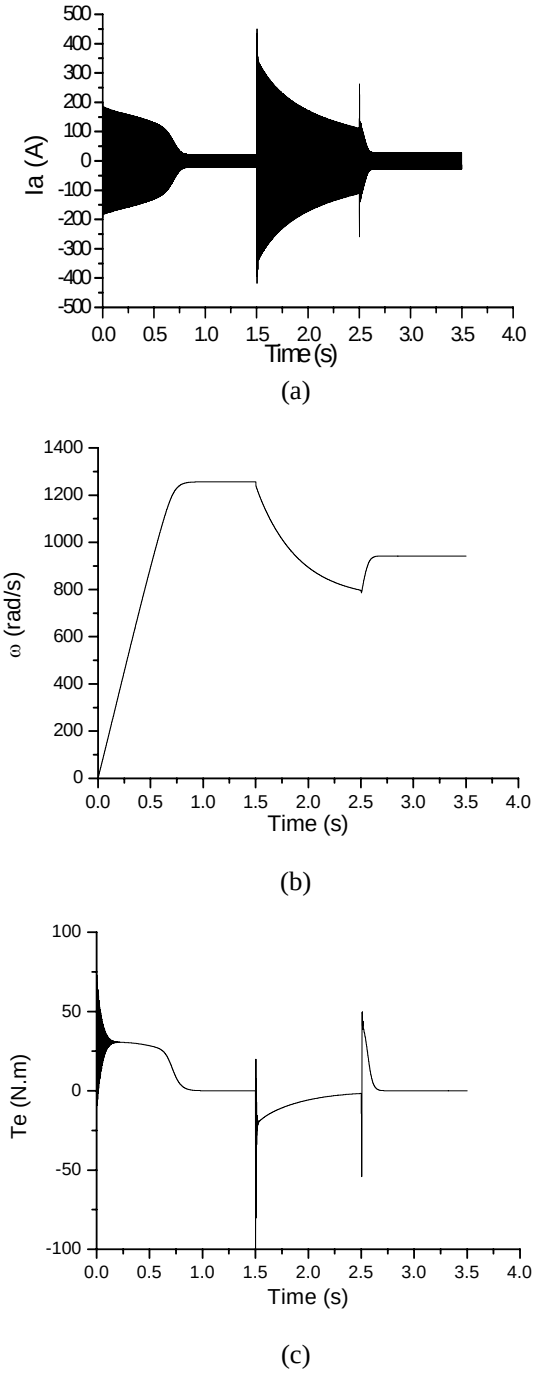

Fig. 11. Dynamic stator current, rotor speed and electromagnetic torque during the period of starting and frequency change.

References

[1] R. Jones, "The More Electric Aircraft: the past and the future," in Electrical Machines and Systems for the More Electric Aircraft (Ref. No. 1999/180), IEE Colloquium on, 1999, pp. 1/1-1/4.

[2] M. Olaiya and N. Buchan, "High power variable frequency generator for large civil aircraft," in Electrical Machines and Systems for the More Electric Aircraft (Ref. No. 1999/180), IEE Colloquium on, 1999, pp. 3/1-3/4.

[3] M. Provost, "The More Electric Aero-engine: a General Overview from an Engine Manufacturer," in Power Electronics, Machines and Drives, 2002. International Conference on (Conf. Publ. No. 487), 2002, pp. 246-251.

[4] C. Avery, et al., "Electrical Generation and Distribution for the More Electric Aircraft," in Universities Power Engineering Conference, 2007. UPEC 2007. 42nd International, 2007, pp. 1007-1012.

[5] W. Cao, et al., "Overview of Electric Motor Technologies Used for More Electric Aircraft (MEA)," Industrial Electronics, IEEE Transactions on, vol. 59, pp. 3523-3531, 2012.

[6] Benarous M. Design of a Direct on-line Induction Motor for Variable Frequency Aerospace Application[J]. 2006.

[7] Environmental Conditions and Test Procedures for Airborne Equipment. 2010 RTCA, Incorporated.

[8] H. Kabbaj, et al., "Skin Effect Characterization in a Squirrel Cage Induction Machine," in Industrial Electronics, 1997. ISIE'97., Proceedings of the IEEE International Symposium on, 1997, pp. 532-536.

[9] W. Levy, et al., "Improved Models for the Simulation of Deep Bar Induction Motors," Energy Conversion, IEEE Transactions on, vol. 5, pp. 393-400, 1990.

[10] O. V. Thorsen and M. Dalva, "A Contribution to the Development of Transient Models for Digital Simulation of Saturated Induction Machines with Deep Bar Effect," in Electrotechnical Conference, 1994. Proceedings. , 7th Mediterranean, 1994, pp. 762-765.

[11] A. C. Smith, et al., "A Transient Induction Motor Model including Saturation and Deep Bar Effect," Energy Conversion, IEEE Transactions on, vol. 11, pp. 8-15, 1996.

[12] J. Li and L. Xu, "Investigation of Cross-saturation and Deep Bar Effects of Induction Motors by Augmented dq Modeling Method," in Industry Applications Conference, 2001. Thirty-Sixth IAS Annual Meeting. Conference Record of the 2001 IEEE, 2001, pp. 745-750.

[13] D. Lin and P. Zhou, "An Improved Dynamic Model for the Simulation of Three-phase Induction Motors with Deep Rotor Bars," in Electrical Machines and Systems, 2008. ICEMS 2008. International Conference on, 2008, pp. 3810-3814.

[14] A.-K. Repo, et al., "Dynamic Electromagnetic Torque Model and Parameter Estimation for a Deep-bar Induction Machine," IET electric power applications, vol. 2, pp. 183-192, 2008.

[15] J. Pedra, et al., "Modelling of Squirrel-cage Induction Motors for Electromagnetic Transient Programs," IET electric power applications, vol. 3, pp. 111-122, 2009.

[16] E. A. Klingshirn and H. E. Jordan, "Simulation of Polyphase Induction Machines with Deep Rotor Bars," Power Apparatus and Systems, IEEE Transactions on, pp. 1038-1043, 1970.

[17] M. Ikeda and T. Hiyama, "Simulation Studies of the Transients of Squirrel-cage Induction Motors," Energy Conversion, IEEE Transactions on, vol. 22, pp. 233-239, 2007.

Xiaofei Du received M.E. degree in electrical engineering from Beihang University, Beijing, China in 2008. He is reading for Ph.D. degree at Beihang University. His research interests include aero electrical power reliability analysis and electrical machine design.

Deqiang Wang received the B.S. and M.S. degrees in electrical engineering from Beihang University, Beijing, China, in 2011 and 2014, respectively. His research interests include aircraft variable-frequency power system, active power filter and motor drive.

Yuanjun Zhou received the B.S. and M.S. degrees in electrical engineering from Beihang University in 1976 and 1982 respectively. She was a visiting scholar at Kyoto University, Japan, from 1986 to 1988. She is a Full Professor of electrical engineering at Beihang University. Her research interests include electric machine design and drive, power converters, and redundant mechanical and electrical control systems.